

# Image Mosaicing for Rolled Fingerprint Construction

Nalini K. Ratha, Jonathan H. Connell and Ruud M. Bolle  
Thomas J. Watson Research Center  
30 Saw Mill River Road  
Hawthorne, NY 10532  
{ratha,jhc,bolle}@watson.ibm.com

## Abstract

With the use of inkless scanners as input devices for acquiring fingerprints of a person, the digital image of the finger is restricted to the area in contact with the sensor. The conventional method of fingerprint image acquisition involves obtaining a nail-to-nail image of the finger known as the rolled fingerprint impression. We present a method of constructing a rolled fingerprint from an image sequence of partial fingerprints using a live-scan fingerprint imager.

## 1. Introduction

Fingerprint-based identification and authentication is one of the most mature and popular biometric techniques used in automatic personal identification [5]. Automating the process of fingerprint identification has been a research topic over several decades. Trained personnel acquire fingerprint impressions of the subject by applying ink on the fingers uniformly and rolling each finger from nail to nail on a paper form. A rolled fingerprint has two advantages: (i) special features like the “delta” points are more readily extractable; (ii) a rolled fingerprint impression covers more area of the finger, hence, has more feature points for representing the finger. As a consequence, any partial fingerprint impression of the same finger will match the rolled print better than it will match another partial fingerprint since the degree of match is related to the amount of overlap.

For these reasons, during enrollment of a person in a large database, a rolled fingerprint would be preferred over a plain touch impression also known as *dab*. A sample rolled fingerprint and a live-scan dab acquired using an optical fingerprint scanner are shown in Figure 1. The main goal of the present work is to reconstruct a rolled fingerprint from a sequence of dabs. As the finger is rolled on the sensor simulating rolling the finger on a paper, an image sequence over the rolling time can be acquired. A sample image sequence is shown in Figure 2.

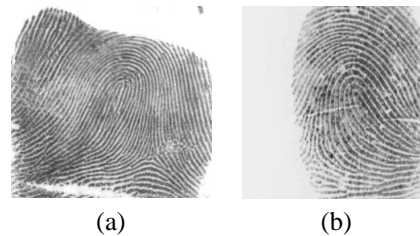


Figure 1. Images. (a) rolled; (b) dab

## 2. Related work

Image mosaicing involves automatic alignment of two or more images into a new aggregate image without any visible seam or distortion in the overlapping areas. Many techniques exist in the literature to construct the scene from a set of images as in satellite image processing [3, 4], medical image analysis, virtual and tele-presence reality [6, 2]. One of the main problems associated with these techniques is their extensive computational requirements because of non-linear optimization techniques used in the algorithms. Often the computational requirements are met with the help of special architectures[1]. The rolled fingerprint construction process is an instance of image mosaicing with the following simplifications: (i) a large number of frames are available covering the fingerprint (the images sequence is being acquired at real-time frame rate of 30 frames a second); (ii) the rolling time period is relatively short so there are no changes in value of the intrinsic and extrinsic imaging parameters; (iii) the rolling is equivalent to rolling a cylindrical surface without slippage, so the images can be considered pre-aligned.

## 3. Proposed scheme

The fingerprint mosaicing algorithm has primarily four stages: (i) segment foreground (fingerprint) and background



**Figure 2. A fingerprint sequence during rolling.**

areas in each frame; (ii) use the foreground mask to weight each image’s contribution; (iii) stack the weighted gray scale frames to compute the mosaiced gray scale image; (iv) stack the foreground masks to compute a confidence index at every pixel.

The first step is to segment each frame into two components: the fingerprint area and the non-fingerprint background area. We are only interested in a rough silhouette of the fingerprint area. We compute a binary image of the fingerprint using a fixed intensity threshold then dilating. Now we have a smoothed blob in each frame representing the fingerprint area in each frame. The foreground and background separation enables us to concentrate only on the fingerprint image characteristics without worrying about the effects of the background. As shown in the upper left corner of Figure 3 naive averaging of the whole set of images introduces substantial washout in the areas where few of the fingerprint images overlap (e.g., sides of the reconstruction).

The next step is to compute the rolled confidence image from the set of foreground masks from each frame. In general, a pixel-wise summation is sufficient for this purpose. This, in a sense, provides the overall spread of our reconstructed rolled fingerprint (i.e., where the confidence is non-zero). In order to construct a rolled fingerprint mosaic, let us visualize the frames stacked as image planes. Assuming that there is no slipping during the rolling, the resultant rolled fingerprint should be aggregate of the individual image components. To achieve this, we look at a pixel  $P(x, y, f_i)$  in all the frames and compute the resultant pixel as a mathematical function of the pixels. An averaging or an order statistics operator can also be considered if the background pixels can be totally eliminated. In Figure 3, we show the results with five different compositing schemes. The simplest approach is naive averaging over the whole image. The next approach neglects the foreground masks altogether and just takes the minimum of the intensity value at each pixel. The third approach averages just in the region where a fingerprint is detected. The fourth approach is similar except that it uses a mask that tapers from 0 at the

edges of the foreground area to 1 when sufficiently close to the center. The fifth approach shrinks the foreground mask so that just the central portion of each fingerprint image is used. This area usually has the best image quality (adequate finger pressure) and the least distortion. The final step is to compute the confidence level at each pixel to evaluate the reconstruction and also to find the region with good confidence. These confidence images are shown next to the reconstructions in Figure 3.

There are several ways to evaluate the different methods as summarized in Table 1. One metric is how large the reconstructed image is in terms of area. The valid areas are determined by looking for non-zero confidence values in the *Foreground*, *Smoothed*, and *Center* methods. For the *Naive* averaging and *Minimum* methods, the first step of foreground processing was used on the composite gray scale image (i.e., threshold and dilate). Since the right side of the *Naive* average image is so faint, it was not considered as foreground and thus this method has the worst score. The area for the *Minimum* method can be considered the best possible case, and is used to normalize the other values. As would be expected, just averaging *Center* regions yields the smallest composite result.

Another way to compare the methods is to judge the quality of the reconstructed images. For instance, the better the contrast in the image, the easier it should be to detect feature points (“minutiae”) for matching. The second column of Table 1 lists the standard deviation of the pixel intensities in the valid areas of the reconstructions. Here the *Minimum* method gives a nice crisp image, with the other methods being somewhat less sharp. Note that the value for *Naive* averaging would be even worse if areas such as the right side of Figure 3 (top) had not already been eliminated by the computed foreground map. A different measure of image quality is signal to noise ratio. Because of the physics of the imaging setup, we do not expect any abrupt changes in pixel values. The ridges on a finger are rounded, not squared off, and the darkness of the impression depends on the microscopic separation of the finger from the imaging plate. To estimate the magnitude of high frequency noise

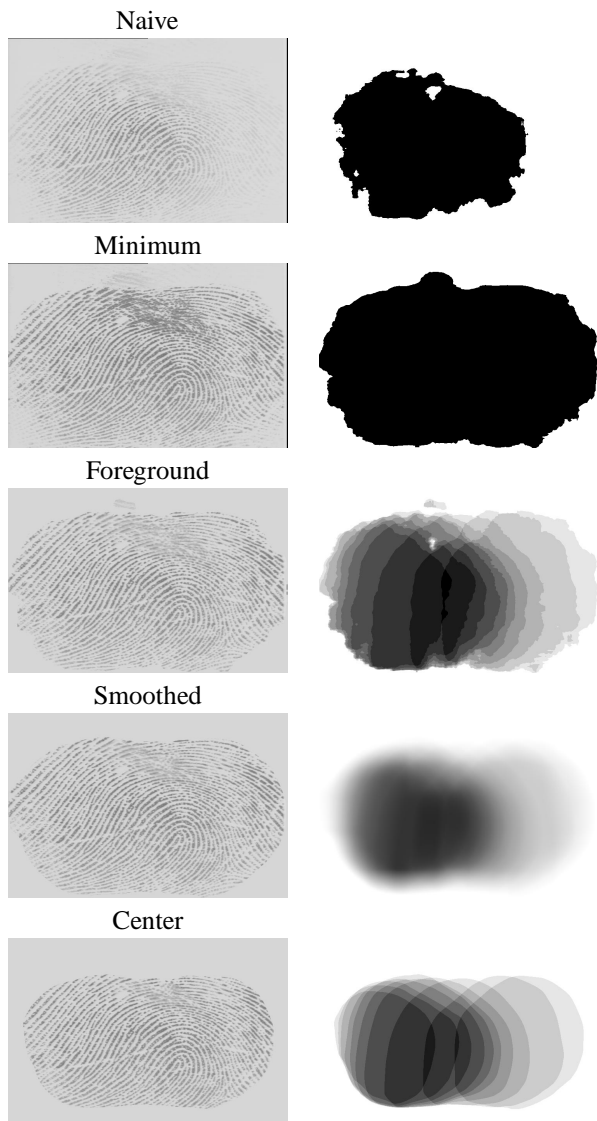


**Figure 3. Result of different compositing schemes. Left image shows results and right image shows confidence levels.**

we compute the edge magnitude at each pixel. That is, we find the average absolute difference of adjacent pixel intensities in the valid areas. The third column in the Table 1 lists the averages for each reconstructed image. Averaging many images obviously reduces noise as seen from the *Naive* value, whereas methods with no averaging such as *Minimum* yield a higher value. The amount of noise can be an important factor if one is attempting to perform parametric fitting of ridges to yield sub-pixel localization.

Finally, the most telling indicator of reconstructed print quality is the number of minutiae extracted. For the sequence in Figure 2 the number of minutiae was determined to be approximately 50 by a human expert. The results of running an automated extraction and pruning procedure on each of the reconstructed images are listed in the fourth col-

	Area	Int. Dev.	Edge Mag.	Minutiae
Naive	33 (18)	23.0 (4.7)	11.1 (2.6)	155 (55)
Min	100 (0)	33.3 (3.9)	15.2 (3.9)	303 (82)
Fgnd	99 (1)	29.8 (3.4)	14.4 (1.8)	243 (62)
Smth	94 (5)	31.2 (3.8)	15.0 (2.1)	222 (43)
Cent	73 (8)	30.6 (3.2)	15.8 (2.3)	163 (43)

**Table 1. Comparative analysis of five methods with standard deviations for 12 prints.**

umn of the table. These values have been normalized by the counts determined by the human expert on the *Center* reconstruction. The *Naive* method misses many of the true minutiae due to the washout phenomenon mentioned earlier. By contrast, the *Minimum* method generates a large number of spurious minutiae. For Figure 3 (second row) these appear mainly around the fuzzy patch near the top center of the reconstruction. The selective averaging methods do better on this patch – more of the ridges are reconstructed as continuous instead of fragmented. In general, the number of minutiae found scales roughly linearly with the reconstructed areas (as is appropriate). Notice that the Center method generates the results closest to ground truth. It does not give rise to any spurious features near the edges of the composite print since it has already removed these poorer quality regions.

## 4. Conclusions

We have demonstrated an effective rolled fingerprint reconstruction technique using image mosaicing. The scheme can handle different types of sensing techniques currently available. There are no assumptions about the image resolution, number of frames or the minimum time for rolling the fingerprint.

## References

- [1] M. Hansen, P. Anandan, K. Dana, G. V. der Wal, and P. Burt. Real-time scene stabilization and mosaic construction. In *Proc. of IEEE Workshop on Applications of Computer Vision, Sarasota, Florida*, pages 54–62, Dec., 1994.
- [2] K. Mase and H. Nishira. Computing the field-of-view of a stitched panorama to create fov sensitive virtual environment. In *Proc. of IAPR Conf. on Pattern Recognition, Lisbon, Portugal*, pages 151–155, Sept. 1996.
- [3] D. L. Milgram. Computer methods for creating photomosaics. *IEEE Trans. on Computers*, 24(11):1113–1119, Nov. 1975.
- [4] D. L. Milgram. Adaptive techniques for photomosaicking. *IEEE Trans. on Computers*, 26(11):1175–1180, Nov. 1977.
- [5] B. Miller. Vital signs of identity. *IEEE Spectrum*, 31(2):22–30, February 1994.
- [6] R. Szelski. Image mosaicing for tele-reality applications. In *Proc. of IEEE Workshop on Applications of Computer Vision, Sarasota, Florida*, pages 44–53, Dec., 1994.